

## Naphthalenyl, Anthracenyl, Tetracenyl, and Pentacenyl Radicals and Their Anions

Brian N. Papas, Suyun Wang, Nathan J. DeYonker, Henry L. Woodcock, and Henry F. Schaefer, III\*

Center for Computational Quantum Chemistry, University of Georgia, Athens, Georgia 30605-2556

Received: April 24, 2003

Electronic structure theory has been applied to the naphthalene-, anthracene-, tetracene-, and pentacene-based radicals and their anions. Five different density functional methods were used to predict adiabatic electron affinities for these radicals. A consistent trend was found, suggesting that the electron affinity at a site of hydrogen removal is primarily dependent upon steric effects for polycyclic aromatic hydrocarbons. The results for the 1-naphthalenyl and 2-naphthalenyl radicals were compared to experiment, and it was found that B3LYP appears to be the most reliable functional for this type of system. For the larger systems the predicted site specific adiabatic electron affinities of the radicals are 1.51 eV (1-anthracenyl), 1.46 eV (2-anthracenyl), and 1.68 eV (9-anthracenyl); 1.61 eV (1-tetracenyl), 1.56 eV (2-tetracenyl), and 1.82 eV (12-tetracenyl); and 1.93 eV (14-pentacenyl), 2.01 eV (13-pentacenyl), 1.68 eV (1-pentacenyl), and 1.63 eV (2-pentacenyl). These electron affinities are 0.5–1.5 eV higher than those for the analogous closed-shell singlet polycyclic aromatic hydrocarbons (PAHs); i.e., EA(anthracene) = 0.53 eV. The global minimum for each radical does not have the same hydrogen removed as the global minimum for the analogous anion. With this in mind, the global (or most preferred site) AEAs are 1.37 eV (naphthalenyl), 1.64 eV (anthracenyl), 1.81 eV (tetracenyl), and 1.97 eV (pentacenyl).

## Introduction

The great stability of polycyclic aromatic hydrocarbons (PAHs) makes them prevalent in our surroundings, and recent research has discussed their abundance in the interstellar medium as well.<sup>1,2</sup> Most notably, PAHs are formed in combustion,<sup>3–5</sup> where they may be precursors to soot<sup>6</sup> and fullerenes.<sup>7</sup> This makes them an important class of pollutants, many of which have been found to be mutagenic and carcinogenic.<sup>8</sup> To better understand their role, PAHs, their radicals, and their anions have been the targets of many recent experimental and theoretical studies.<sup>9–16</sup>

The PAHs examined in this study are derived from naphthalene (C<sub>10</sub>H<sub>8</sub>), anthracene (C<sub>14</sub>H<sub>10</sub>), tetracene (C<sub>18</sub>H<sub>12</sub>), and pentacene (C<sub>22</sub>H<sub>14</sub>). All unique radicals formed by homolytically splitting a carbon–hydrogen bond are studied, as well as the anions of those radicals. The primary focus of this paper is the electron affinities (EAs) of the aryl radicals. See Figure 1 for the standard numbering of the carbon atoms.

Recent experimental studies have determined EAs for the naphthalenyl radicals.<sup>9–11</sup> These results will be used as a basis for judging the accuracy of several density functionals. The PAHs and their radicals, but not their anions, have been the subject of important DFT studies by Cioslowski<sup>13,14</sup> and Wiberg.<sup>15</sup> Average theoretical errors in EAs for PAHs and other molecules, as found by Rienstra-Kiracofe, Tschumper, Schaefer, Nandi, and Ellison,<sup>16</sup> shall be used for evaluating the reliability of our results.

## Methods

All computations employed a double- $\zeta$  basis set with polarization and diffuse functions, denoted DZP++. Previous work<sup>17,18</sup> has shown that this basis has the flexibility needed for accurate results, while maintaining a small size appropriate

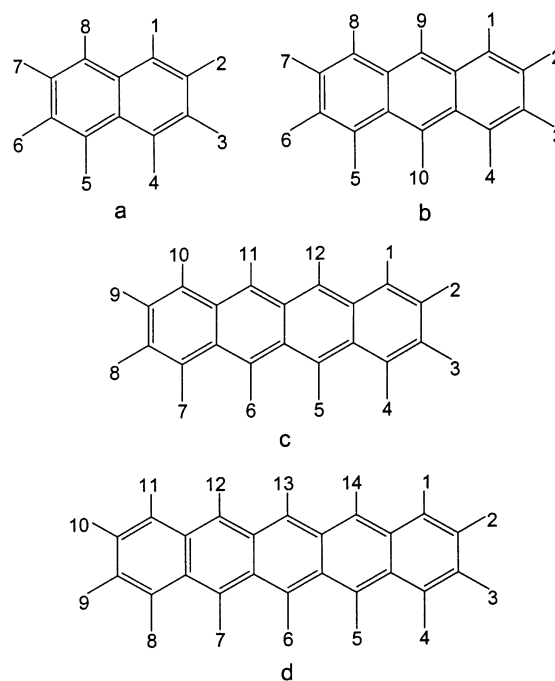


**Figure 1.** IUPAC numbering scheme for (a) naphthalene, (b) anthracene, (c) tetracene, and (d) pentacene.

for larger molecular systems. It was constructed by augmenting the Huzinaga–Dunning<sup>19,20</sup> set of contracted double- $\zeta$  Gaussian functions with one set of p polarization functions for each hydrogen atom and one set of d polarization functions for each carbon atom [4s2p1d|2s1p] ( $\alpha_p(\text{H}) = 0.75$ ,  $\alpha_d(\text{C}) = 0.75$ ). To complete the DZP++ basis, one diffuse s function was added to each hydrogen atom, and a set of diffuse s and p functions to each carbon atom. These diffuse “even-tempered” orbital

exponents were determined according to the guidelines of Lee and Schaefer.<sup>21</sup> That is, the s- or p-type diffuse function exponent,  $\alpha_{\text{diffuse}}$ , for a given atom was determined by

$$\alpha_{\text{diffuse}} = \frac{1}{2} \left( \frac{\alpha_1}{\alpha_2} + \frac{\alpha_2}{\alpha_3} \right) \alpha_1 \quad (1)$$

where  $\alpha_1$  is the smallest,  $\alpha_2$  the second smallest, and  $\alpha_3$  the third smallest Gaussian orbital exponent of the s- or p-type primitive functions of that atom [ $\alpha_{\text{S}}(\text{H}) = 0.04415$ ,  $\alpha_{\text{S}}(\text{C}) = 0.04302$ ,  $\alpha_{\text{P}}(\text{C}) = 0.03629$ ]. All polarization and diffuse orbital exponents were unscaled. There are a total of 6 DZP++ contracted Gaussian basis functions/hydrogen atom and 19/carbon atom.

Five different exchange-correlation density functionals were used to determine the electronic energies, equilibrium geometries, harmonic vibrational frequencies, and zero-point vibrational energies (ZPVEs) for the naphthalene-, anthracene-, and tetracene-derived radicals and anions. The functionals that were used have been denoted B3LYP, B3LYP, BLYP, BP86, and LSDA. Only the B3LYP functional was used for pentacene. All but LSDA are generalized gradient approximations (GGAs) and employ either the dynamical correlation functional of Lee, Yang, and Parr (LYP)<sup>22</sup> or that of Perdew (P86)<sup>23,24</sup> in conjunction with one of Becke's exchange functionals: the three-parameter HF/DFT hybrid exchange functional (B3),<sup>25</sup> a modification of the half-and-half HF/DFT hybrid method (BH)<sup>26</sup> (the BH functional as implemented in Gaussian 94<sup>27</sup>) or the 1988 pure DFT exchange functional (B).<sup>28</sup> The final density functional scheme used in this study was the standard local-spin-density approximation (LSDA) which employs the 1980 correlation functional of Vosko, Wilk, and Nusair<sup>29</sup> along with the Slater exchange functional.<sup>30–32</sup>

The quantum chemical computations of the naphthalene and anthracene derived species were conducted using the Gaussian 94<sup>26</sup> computational package, while the tetracene- and pentacene-derived species were done using the Gaussian 98<sup>33</sup> computational package. Spin unrestricted Kohn–Sham orbitals were used for all computations. Both the neutral and anion geometries were fully optimized via analytic gradients with each of the density functionals. Numerical integration of the functions was carried out using the Gaussian 94<sup>26</sup> and 98<sup>33</sup> default grid consisting of 75 radial shells and 302 angular points per shell. The mass-weighted Hessian matrix, and hence the harmonic vibrational frequencies, were determined analytically for all DFT methods for the naphthalenyl, anthracenyl, and tetracenyl species. ZPVE corrections for pentacenyl energies were approximated by extrapolating a linear trend in ZPVE corrections with respect to number of rings from the results of the other PAHs.

The electron affinities (AEAs) in this report are all adiabatic and have values determined by

$$\text{AEA} = E_{\text{neutral}} - E_{\text{anion}} \quad (2)$$

where the geometry of each species is optimized independently for local AEAs. Global AEAs are also determined, where the global energy minimum for each species is used. An alternate term for “global EA” is “most preferred site EA”. The global EA is the energy difference between the lowest energy isomer of the radical and the lowest energy isomer of the anion. Corrections for zero-point vibrational energies were computed by adding the ZPVE correction to each energy before determining the EA. A positive EA corresponds to a bound electron. In this study, all species were optimized with the “tight” conver-

**TABLE 1: *Ipsa* C–C–C Angles (in deg) for the Radicals and Their Anions**

		B3LYP	BLYP	BHLYP	BP86	LSDA
1-naphthalenyl	radical	126.6	126.7	126.4	126.7	126.9
	symmetry	C <sub>s</sub>	C <sub>s</sub>	C <sub>s</sub>	C <sub>s</sub>	C <sub>s</sub>
	anion	112.6	112.8	112.6	112.5	112.8
2-naphthalenyl	radical	126.3	126.3	126.1	126.4	126.7
	symmetry	C <sub>s</sub>	C <sub>s</sub>	C <sub>s</sub>	C <sub>s</sub>	C <sub>s</sub>
	anion	111.9	112.0	111.9	111.7	112.2
1-anthracenyl	radical	126.8	126.9	126.5	126.9	127.1
	symmetry	C <sub>s</sub>	C <sub>s</sub>	C <sub>s</sub>	C <sub>s</sub>	C <sub>s</sub>
	anion	112.6	112.6	112.6	112.3	112.7
2-anthracenyl	radical	126.5	126.5	126.3	126.6	126.9
	symmetry	C <sub>s</sub>	C <sub>s</sub>	C <sub>s</sub>	C <sub>s</sub>	C <sub>s</sub>
	anion	111.9	112.5	112.0	112.7	114.3
9-anthracenyl	radical	127.3	127.6	127.0	127.5	127.7
	symmetry	C <sub>s</sub>	C <sub>s</sub> '	C <sub>s</sub> '	C <sub>s</sub> '	C <sub>s</sub> '
	anion	113.4	113.6	113.3	113.2	113.5
1-tetracenyl	radical	126.8	126.9	126.6	127.0	127.2
	symmetry	C <sub>s</sub>	C <sub>2v</sub>	C <sub>2v</sub>	C <sub>2v</sub>	C <sub>2v</sub>
	anion	112.5	112.7	112.6	112.3	112.7
2-tetracenyl	radical	126.5	126.6	126.2	126.7	126.9
	symmetry	C <sub>s</sub>	C <sub>s</sub>	C <sub>s</sub>	C <sub>s</sub>	C <sub>s</sub>
	anion	112.0	112.0	112.1	111.8	112.7
12-tetracenyl	radical	127.5	127.7	127.1	127.7	127.8
	symmetry	C <sub>s</sub>	C <sub>s</sub>	C <sub>s</sub>	C <sub>s</sub>	C <sub>s</sub>
	anion	113.4	113.5	113.4	113.2	113.4
1-pentacenyl	radical	126.9				
	symmetry	C <sub>s</sub>				
	anion	112.6				
2-pentacenyl	radical	126.6				
	symmetry	C <sub>s</sub>				
	anion	112.1				
13-pentacenyl	radical	127.6				
	symmetry	C <sub>2v</sub>				
	anion	113.3				
14-pentacenyl	radical	127.6				
	symmetry	C <sub>s</sub>				
	anion	113.4				
	symmetry	C <sub>s</sub>				

gence criterion in the DFT frame using the Gaussian 94<sup>26</sup> or Gaussian 98<sup>33</sup> packages.

## Results and Discussion

It should first be noted that the addition of diffuse functions has a significant impact upon the energetics. Sample B3LYP calculations on the 9-anthracenyl species showed a lowering of about 6 kcal/mol for the radical and 13 kcal/mol for the anion when the diffuse functions were added. The geometries were not significantly different.

Another concern is that of comparing Gaussian 94<sup>26</sup> results with those from Gaussian 98.<sup>33</sup> To address this concern, a B3LYP computation was performed on the 9-anthracenyl species. ZPVE-corrected EAs were found to be different by less than 0.005 eV. As such, comparisons of EAs between the two versions should be valid.

One possible gauge of the accuracy of the results is an evaluation of  $\langle S^2 \rangle$ . For the radicals studied, this would be 0.75 in a spin-restricted formalism. For anthracenyl, BHLYP gives

TABLE 2: C–C Bond Lengths (in Å) Adjacent to the Removed Hydrogen Atom

			B3LYP	BLYP	BHLYP	BP86	LSDA
1-naphthalenyl	radical	left	1.407	1.414	1.401	1.411	1.395
		right	1.364	1.375	1.353	1.372	1.359
	anion	left	1.451	1.460	1.443	1.457	1.437
		right	1.407	1.417	1.396	1.415	1.399
2-naphthalenyl	radical	left	1.364	1.375	1.353	1.372	1.358
		right	1.404	1.411	1.398	1.408	1.392
	anion	left	1.405	1.416	1.393	1.414	1.397
		right	1.449	1.457	1.442	1.454	1.435
1-anthracenyl	radical	left	1.415	1.421	1.411	1.417	1.401
		right	1.357	1.369	1.346	1.367	1.353
	anion	left	1.461	1.469	1.455	1.464	1.444
		right	1.400	1.412	1.388	1.410	1.394
2-anthracenyl	radical	left	1.357	1.369	1.346	1.367	1.353
		right	1.413	1.419	1.409	1.415	1.399
	anion	left	1.399	1.409	1.385	1.406	1.386
		right	1.459	1.463	1.453	1.456	1.430
9-anthracenyl	radical	left	1.386	1.395	1.379	1.393	1.378
		right	1.386	1.395	1.379	1.393	1.378
	anion	left	1.431	1.441	1.421	1.438	1.420
		right	1.431	1.441	1.421	1.438	1.420
1-tetracenyl	radical	left	1.419	1.424	1.411	1.420	1.403
		right	1.355	1.367	1.348	1.365	1.351
	anion	left	1.465	1.472	1.460	1.468	1.446
		right	1.398	1.410	1.385	1.408	1.392
2-tetracenyl	radical	left	1.354	1.367	1.348	1.365	1.351
		right	1.417	1.423	1.410	1.419	1.402
	anion	left	1.397	1.410	1.382	1.407	1.446
		right	1.464	1.472	1.460	1.467	1.392
12-tetracenyl	radical	left	1.396	1.403	1.390	1.400	1.385
		right	1.379	1.389	1.377	1.387	1.372
	anion	left	1.442	1.451	1.434	1.448	1.429
		right	1.424	1.435	1.413	1.433	1.415
1-pentacenyl	radical	left	1.420				
		right	1.354				
	anion	left	1.466				
		right	1.397				
2-pentacenyl	radical	left	1.353				
		right	1.419				
	anion	left	1.396				
		right	1.466				
13-pentacenyl	radical	left	1.389				
		right	1.389				
	anion	left	1.435				
		right	1.436				
14-pentacenyl	radical	left	1.400				
		right	1.377				
	anion	left	1.448				
		right	1.421				

the largest deviation, with the 9-anthracenyl radical value being 0.85. All  $\langle S^2 \rangle$  values for the other radicals were below 0.77. This suggests reasonable results, though it should be noted, as by Pople, Gill, and Handy,<sup>34</sup> that the DFT determinant formed from spin-orbitals is not a true wave function and  $\langle S^2 \rangle$  is not necessarily meaningful.

Vibrational frequencies were evaluated to confirm minimum energy structures and to determine ZPVEs. In all cases, structures were found for stable energy minima. It is worth noting that several anthracenyl species broke the expected symmetry, as well as one of the pentacenyl (see Tables 1 and 2). Note that the 9-anthracenyl radical should have  $C_{2v}$  symmetry, while the 2-anthracenyl radical should have  $C_s$  symmetry, but several functionals gave lower symmetries. For instance, the B3LYP computations gave a 9-anthracenyl anion geometry in which the hydrogens remain in one plane but are not symmetric with respect to the bisecting plane which contains the 9 site. This  $C_s$  symmetry, however, is energetically and geometrically very close to the nearest  $C_{2v}$  symmetry. This suggests that the symmetry loss is not physical but instead an

artifact of the computation method, most probably due to the numerical integration procedures necessary in DFT methods.

The majority of the change in geometry upon the addition of the  $\sigma$  electron occurs at the site of the hydrogen removal. Relevant parameters are the carbon-carbon-carbon angle associated with the site of removal (the *ipso* angle) and the carbon-carbon bond lengths adjacent to the site. The “left” and “right” labels in Table 2 refer to the position of the bond relative to the site of the removed hydrogen in the IUPAC orientation. In the designation of symmetries,  $C_s$  refers to a system where the plane of symmetry contains all of the atoms, while  $C_s'$  bisects the middle ring.

On average, the *ipso* bond angle decreases by  $14^\circ$  and the adjacent bond lengths increase by 0.04 Å with the addition of the last electron. The angle change is consistent with the results found by Ervin et al.<sup>9</sup> using Gaussian 98<sup>33</sup> and a B3LYP/aug-cc-pVDZ computation for the smaller naphthalenyl species. The geometry changes are highly consistent between different PAH-derived radicals. In fact, when comparing similar radicals (1-naphthalenyl to 1-anthracenyl and 2-naphthalenyl to 2-anthra-

**TABLE 3: EAs (in eV) with ZPVE-Corrected Values in Parentheses**

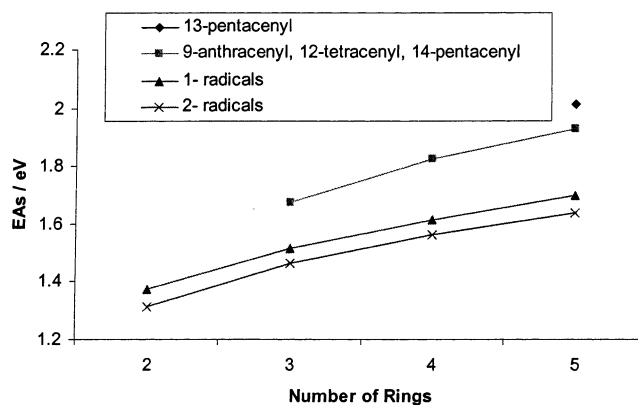
	B3LYP	BHLYP	BLYP	BP86	LSDA	expt 1	expt 2	expt 3
1-naphthalenyl	1.31 (1.37)	1.06 (1.11)	1.24 (1.30)	1.40 (1.47)	1.97 (2.03)	1.37 ± 0.02	1.43 ± 0.06	1.403 ± 0.015
2-naphthalenyl	1.25 (1.31)	0.99 (1.04)	1.19 (1.25)	1.35 (1.42)	1.90 (1.96)	1.30 ± 0.02	1.37 ± 0.04	1.34 <sup>+0.03</sup> <sub>-0.07</sub>
1-anthracenyl	1.46 (1.51)	1.19 (1.24)	1.38 (1.45)	1.56 (1.62)	2.12 (2.18)			
2-anthracenyl	1.39 (1.46)	1.12 (1.17)	1.33 (1.41)	1.51 (1.58)	2.07 (2.15)			
9-anthracenyl	1.61 (1.68)	1.37 (1.42)	1.51 (1.58)	1.69 (1.77)	2.28 (2.35)			
1-tetracenyl	1.55 (1.61)	1.25 (1.27)	1.48 (1.53)	1.66 (1.71)	2.22 (2.27)			
2-tetracenyl	1.49 (1.56)	1.17 (1.20)	1.43 (1.48)	1.60 (1.65)	2.15 (2.20)			
12-tetracenyl	1.75 (1.82)	1.47 (1.49)	1.65 (1.72)	1.84 (1.91)	2.43 (2.49)			
1-pentacenyl	1.61 (1.68)							
2-pentacenyl	1.55 (1.63)							
13-pentacenyl	1.93 (2.01)							
14-pentacenyl	1.84 (1.93)							

cenyl, etc.), one finds that the *ipso* angle is usually different by at most 0.2° and the bond lengths are different by 0.01 Å. The exceptions to this trend involve anthracenyl systems which broke symmetry. This suggests that the behaviors of the radical and its anion are relatively independent of the total system—what matters is that it is part of a PAH.

Theoretical EAs are reported in Table 3. ZPVE-corrected EAs appear in parentheses. The ZPVE correction is typically around 0.06 eV for the naphthalenyl radicals, 0.07 eV for the anthracenyl radicals, and 0.05 eV for the tetracenyl radicals (the BHLYP corrections are very small compared to the others). On average, the 1-naphthalenyl radical has an EA approximately 0.06 eV higher than the 2-naphthalenyl radical. This difference is in good agreement with the values reported from experiment.<sup>9–11</sup> The difference between the 1-anthracenyl radical EA and the 2-anthracenyl radical EA is on average 0.05 eV, though the different functionals predict a wider range of values. The same separation for the tetracenyl radical EA is 0.06 eV. The highest EA for anthracenyl is that of the 9-anthracenyl radical structure, which is on average 0.16 eV higher than the value for the 1-anthracenyl radical. The highest EA for the tetracenyl radical is that of the 12-tetracenyl radical, which is 0.21 eV higher than the 1-tetracenyl radical EA. The highest EA for the pentacenyl radical is that of the 13-pentacenyl radical, which is 0.33 eV higher than the value for the 1-pentacenyl radical.

Combining the results of experiments by Reed and Kass,<sup>10</sup> Lardin et al.,<sup>11</sup> and Ervin et al.<sup>9</sup> gives average values for the EAs of the naphthalenyl radicals. The EA of the 1-naphthalenyl radical is 1.40 eV, and that of the 2-naphthalenyl radical is 1.34 eV. Compared to these, the smallest average error among the functionals is that for B3LYP, an error of 0.03 eV. This is much smaller than the average error of 0.14 eV reported by Rienstra-Kiracofe et al.<sup>15</sup> in their systematic study of 91 EAs. Also close are BLYP and BP86, which have errors of 0.10 and 0.08 eV, respectively, for the naphthalenyl radicals. The remaining functionals, BHLYP and LSDA, compare poorly, with LSDA far off from experimental value by any means of comparison. This suggests that the B3LYP values for the anthracenyl and tetracenyl radicals are the ones that should be considered the best, and this is the reason only B3LYP was used for the pentacene based species.

There are four main points to consider for the energetics studies: the energetic ordering of the radicals; the ordering of the anions; the ordering of the local EAs; the ordering of the global EAs. In Table 4, each energy is reported relative to the minimum for the functional and the given parent PAH. For all but the BLYP computation, the 2-naphthalenyl radical is more stable than the 1-naphthalenyl radical. However, if we ignore the presumably inaccurate LSDA results, the largest radical separation is only 0.13 kcal/mol. This separation is so small that it should not be considered significant.

**Figure 2.** EAS vs number of rings.**TABLE 4: ZPVE-Corrected Energies (kcal/mol) Relative to Lowest Energy Species**

		B3LYP	BHLYP	BLYP	BP86	LSDA
1-naphthalenyl	radical	31.647	25.663	29.995	33.874	46.717
	anion	0.000	0.000	0.000	0.000	0.000
2-naphthalenyl	radical	31.569	25.530	30.005	33.824	46.325
	anion	1.273	1.499	1.131	1.159	1.144
1-anthracenyl	radical	38.057	32.393	36.006	40.192	53.175
	anion	3.124	3.768	2.663	2.771	2.843
2-anthracenyl	radical	37.925	32.224	35.958	40.089	52.732
	anion	4.219	5.156	3.413	3.555	3.124
9-anthracenyl	radical	38.629	32.819	36.529	40.711	54.105
	anion	0.000	0.000	0.000	0.000	0.000
1-tetracenyl	radical	41.822	34.383	39.244	43.551	56.543
	anion	4.597	5.153	3.935	4.083	4.094
2-tetracenyl	radical	41.758	34.323	39.288	43.527	56.145
	anion	5.773	6.724	5.111	5.375	5.470
12-tetracenyl	radical	42.077	34.383	39.660	43.984	57.409
	anion	0.000	0.000	0.000	0.000	0.000
1-pentacenyl	radical	46.333				
	anion	7.525				
2-pentacenyl	radical	46.325				
	anion	8.674				
13-pentacenyl	radical	46.429				
	anion	0.000				
14-pentacenyl	radical	45.814				
	anion	1.319				

Among the anthracenyl radicals, the 9-species is consistently the highest in electronic energy. This is followed by the 1-anthracenyl radical and then the 2-anthracenyl radical. It should be noted, however, that (except for LSDA) the total range of energies for the radicals is at most 0.7 kcal/mol. Except for BLYP, the tetracenyl radicals show ordering similar to the anthracene-based radicals. The difference is that BLYP predicts the 1-tetracenyl radical to lie energetically lower than the 2-tetracenyl radical. Once again, the separation of the 1- and 2-radicals is so small (0.11 kcal/mol at most, ignoring LSDA) that we should view the two structures as energetically degenerate.

TABLE 5: Global AEAs (eV) with ZPVE-Corrected Values in Parentheses

	B3LYP	BHLYP	BLYP	BP86	LSDA
naphthalenyl	1.31 (1.37)	1.05 (1.11)	1.24 (1.30)	1.40 (1.47)	1.95 (2.01)
anthracenyl	1.59 (1.64)	1.36 (1.40)	1.50 (1.56)	1.68 (1.74)	2.24 (2.29)
tetracenyl	1.74 (1.81)	1.47 (1.49)	1.64 (1.70)	1.83 (1.89)	2.38 (2.43)
pentacenyl	1.89 (1.99)				

ate. The pentacenyl radicals are in an energy ordering comparable to anthracenyl and tetracenyl. The least stable radical is 13-pentacenyl, followed by 1-pentacenyl and then 2- and 14-pentacenyl. The energies span a range of 0.62 kcal/mol for the anthracenyl radicals and 0.31 kcal/mol for the tetracenyl radicals (both ignoring LSDA), again very small numbers.

For the naphthalene-based systems, the 1-naphthalenyl anion is consistently the most stable. It is, on average, 1.24 kcal/mol more stable than the 2-anion. The ordering of the anthracenyl anions is also consistent between all functionals: the 9-anthracenyl anion is the most stable, with the 1-anthracenyl anion more stable than the 2-anthracenyl anion. This ordering is sensible, since the electron cloud corresponding to the additional electron (which has no associated H-atom) experiences greater electron–electron repulsion in species with more hydrogens near the site of the hydrogen removal. Specifically, the 9-site of the anthracenyl radical has no hydrogens on adjacent carbons, the 1-site one, and the 2-site two. The tetracenyl anions show the same trend, with the 12-species the most stable, followed by the 1- and then the 2-, and the pentacenyl anions are also consistent, falling in the order of 13-, 14-, 1-, and then 2-.

One reviewer has proposed an alternate explanation. Since the hybridization of the anionic center must have more s character (s orbitals are closer to the nucleus) the ipso C–C bonds must have more p character. This means that the bond angle must decrease, as is seen in the theoretical predictions. This deformation causes significant strain, and it is the ability of the particular anionic site to accommodate this strain that determines the relative energies. While this certainly explains the change in the C–C–C angle, the neighboring hydrogen atoms in the 1- and 2-anthracenyl anions are bent away from the anionic site, in one case by 5°. This suggests the presence of steric effects in addition to hybridization effects.

As noted, the radicals have small energetic separations. So small, in fact, that the ordering of the EAs of the various species is almost entirely dependent upon the ordering of the anions. The EAs, then, fall in order according to steric and hybridization effects, just like the anions.

Figure 2 details the changes in the EAs as the number of rings involved increases. The trends seem to be near linear, with the increase in EA decreasing slightly with each ring added. In general, larger ring systems have greater EAs for comparable radicals (the 1-radicals, 2-radicals, and 9-anthracenyl with 12-tetracenyl and 14-pentacenyl and 13-pentacenyl by itself). It is likely that the larger ring systems allow the electron density around the site of the last electron to spread out more, thus stabilizing the anion.

Table 5 gives predicted values for the global EAs. In all cases the trend is simple—the global EA increases as the number of rings increases. This most likely occurs for the same reason as the trend in the local EAs—the larger ring system stabilizes the anions more. Since the radicals for each set of systems with the same number of rings are so close together in energy, the global EA depends almost exclusively upon this stabilization effect.

## Conclusions

Potential surface minima, harmonic vibrational frequencies, and EAs have been computed for naphthalene-, anthracene-,

and tetracene-based radicals using five different density functionals. All except vibrational frequencies were found for pentacene-based radicals using only B3LYP. Optimized geometries are reported, and the geometry changes with electron attachment are consistent for all functionals. It would also appear that the relative order of EAs for different sites within a given PAH is mainly dependent upon steric effects and perhaps upon hybridization effects as well. Which is more significant could be pursued further by placing larger groups adjacent to the site of hydrogen removal. In addition, both the local EAs for equivalent radical sites and the global EAs increased as the number of rings in the system increased.

Results for the 1- and 2-naphthalenyl radicals have been compared to experiment, and the most accurate functional was found to be B3LYP. BLYP and BP86 are also in good agreement with experiment. As such, those three functionals are recommended for use on future computational studies of PAHs.

**Acknowledgment.** This research was supported by the U.S. Department of Energy Combustion and SciDAC programs. Computations using GAUSSIAN 98 were carried out at the NERSC (National Energy Research Supercomputing Center) at the Lawrence Berkeley Laboratory, also supported by the Department of Energy. We thank Dr. Zhi-Xiang Wang for many helpful discussions.

## References and Notes

- (1) Cook, D. J.; Saykally, R. J. *Astrophys. J.* **1998**, *493*, 793.
- (2) Szczepanski, J.; Vala, M. *Nature* **1993**, *363*, 699.
- (3) Wang, H.; Frenklach, M. *J. Phys. Chem.* **1994**, *98*, 11465.
- (4) Richter, H.; Mazyar, O. A.; Sumathi, R.; Green, W. H.; Howard, J. B.; Bozzelli, J. W. *J. Phys. Chem. A* **2001**, *105*, 1561.
- (5) Barckholtz, C.; Barckholtz, T. A.; Hadad, C. M. *J. Am. Chem. Soc.* **1999**, *121*, 491.
- (6) Calcote, H. F. *Combust. Flame* **1981**, *42*, 215.
- (7) Pope, C. J.; Marr, J. A.; Howard, J. B. *J. Phys. Chem.* **1993**, *97*, 11001.
- (8) Durant, J. L.; Busby, W. F.; Lafleur, A. L.; Penman, B. W.; Crespi, C. L. *Mutat. Res.* **1996**, *371*, 123.
- (9) Ervin, K. M.; Ramond, T. M.; Davico, G. E.; Schwartz, R. L.; Casey, S. M.; Lineberger, W. C. *J. Phys. Chem. A* **2001**, *105*, 10822.
- (10) Reed, D. R.; Kass, S. R. *J. Mass Spectrom.* **2000**, *35*, 534.
- (11) Lardin, H. A.; Squires, R. R.; Wenthold, P. G. *J. Mass Spectrom.* **2001**, *36*, 607.
- (12) Wong, M. W. *Chem. Phys. Lett.* **1996**, *256*, 391.
- (13) Cioslowski, J.; Liu, G. H.; Martinov, M.; Piskorz, P.; Moncrieff, D. *J. Am. Chem. Soc.* **1996**, *118*, 5261–5264.
- (14) Cioslowski, J.; Liu, G. H.; Moncrieff, D. *J. Org. Chem.* **1996**, *61*, 4111.
- (15) Wiberg, K. B. *J. Org. Chem.* **1997**, *62*, 5720–5727.
- (16) Rienstra-Kiracofe, J. C.; Tschumper, G. S.; Schaefer, H. F.; Nandi, S.; Ellison, G. B. *Chem. Rev.* **2002**, *102*, 231–282.
- (17) Brown, S. T.; Rienstra-Kiracofe, J. C.; Schaefer, H. F. *J. Phys. Chem. A* **1999**, *103*, 4065.
- (18) Rienstra-Kiracofe, J. C.; Barden, C. J.; Brown, S. T.; Schaefer, H. F. *J. Phys. Chem. A* **2001**, *105*, 524.
- (19) Huzinaga, S. *J. Chem. Phys.* **1965**, *42*, 1293.
- (20) Dunning, T. H., *J. Chem. Phys.* **1970**, *53*, 2823.
- (21) Lee, T. J.; Schaefer, H. F. *J. Chem. Phys.* **1985**, *83*, 1784.
- (22) Lee, C.; Yang, W.; Parr, R. G. *Phys. Rev. B* **1998**, *37*, 785.
- (23) Perdew, J. P. *Phys. Rev. B* **1986**, *33*, 8822.
- (24) Perdew, J. P. *Phys. Rev. B* **1986**, *34*, 7406.
- (25) Becke, A. D. *J. Chem. Phys.* **1993**, *98*, 5648.
- (26) Becke, A. D. *J. Chem. Phys.* **1992**, *98*, 1372.

(27) Frisch, M. J.; Trucks, G. W.; Schlegel, H. B.; Gill, P. M. W.; Johnson, B. G.; Robb, M. A.; Cheeseman, J. R.; Keith, T.; Petersson, G. A.; Montgomery, J. A.; Raghavachari, K.; Al-Laham, M. A.; Zakrzewski, V. G.; Ortiz, J. V.; Foresman, J. B.; Cioslowski, J.; Stefanov, B. B.; Nanayakkara, A.; Challacombe, M.; Peng, C. Y.; Ayala, P. Y.; Chen, W.; Wong, M. W.; Andres, J. L.; Replogle, E. S.; Gomperts, R.; Martin, R. L.; Fox, D. J.; Binkley, J. S.; Defrees, D. J.; Baker, J.; Stewart, J. P.; Head-Gordon, M.; Gonzalez, C.; Pople, J. A. *Gaussian 94*, revision E.2; Gaussian, Inc.: Pittsburgh, PA, 1995.

(28) Becke, A. D. *Phys. Rev. A* **1998**, 38, 3098.

(29) Vosko, S. H.; Wilk, L.; Nusair, M.; *Can. J. Phys.* **1980**, 58, 1200.

(30) Hohenberg, P.; Kohn, W. *Phys. Rev. A* **1964**, 136, 864.

(31) Kohn, W.; Sham, L. J. *Phys. Rev. A* **1965**, 140, 1133.

(32) Slater, J. C. *Quantum Theory of Molecules and Solids: The Self-Consistent Field for Molecules and Solids*; McGraw-Hill: New York, 1974; Vol. IV.

(33) Frisch, M. J.; Trucks, G. W.; Schlegel, H. B.; Scuseria, G. E.; Robb, M. A.; Cheeseman, J. R.; Zakrzewski, V. G.; Montgomery, J. A., Jr.; Stratmann, R. E.; Burant, J. C.; Dapprich, S.; Millam, J. M.; Daniels, A. D.; Kudin, K. N.; Strain, M. C.; Farkas, O.; Tomasi, J.; Barone, V.; Cossi, M.; Cammi, R.; Mennucci, B.; Pomelli, C.; Adamo, C.; Clifford, S.; Ochterski, J.; Petersson, G. A.; Ayala, P. Y.; Cui, Q.; Morokuma, K.; Malick, D. K.; Rabuck, A. D.; Raghavachari, K.; Foresman, J. B.; Cioslowski, J.; Ortiz, J. V.; Stefanov, B. B.; Liu, G.; Liashenko, A.; Piskorz, P.; Komaromi, I.; Gomperts, R.; Martin, R. L.; Fox, D. J.; Keith, T.; Al-Laham, M. A.; Peng, C. Y.; Nanayakkara, A.; Gonzalez, C.; Challacombe, M.; Gill, P. M. W.; Johnson, B. G.; Chen, W.; Wong, M. W.; Andres, J. L.; Head-Gordon, M.; Replogle, E. S.; Pople, J. A. *Gaussian 98*, revision A.11; Gaussian, Inc.: Pittsburgh, PA, 1998.

(34) Pople, J. A.; Gill, P. M. W.; Handy, N. C. *Int. J. Quantum Chem.* **1995**, 56, 303.